

Microwave-assisted polyol synthesis of sub-micrometer Y_2O_3 and $\text{Yb-Y}_2\text{O}_3$ particles for laser source application

Marina Serantoni ^{*}, Elisa Mercadelli, Anna Luisa Costa, Magda Blosi,
Laura Esposito, Alessandra Sanson

Institute of Science and Technology for Ceramic (ISTEC), National Research Council (CNR), Via Granarolo 64, I-48018 Faenza (RA), Italy

Received 8 May 2009; received in revised form 7 June 2009; accepted 1 July 2009

Available online 17 July 2009

Abstract

Sub-micrometer powder (100–150 nm diameter) of Yb-doped yttrium oxide was obtained, for the first time, by microwave-assisted polyol (diethylene glycol, DEG) method. This method is based on fast and homogeneous increase of temperature, due to the microwave heating, and on addition of the hydrolysing agent (water) at high temperature. This promotes a fast nucleation followed by a controlled growth of nuclei. Different procedures were used to process the as-synthesized powders. In some cases washing by ultrapure water was used to dissolve nitrate and DEG by-products, this treatment allowed the use of a lower calcination temperature (150–200 °C less) to obtain the crystalline phase. Analysis of the calcined powder showed different levels of structures: from nanocrystal (10–15 nm), to primary particles (100–150 nm), to micrometer soft aggregates (2–4 μm). The microwave-assisted polyol method resulted an easy way to dope yttria with the desired amount of Yb^{3+} . This work was carried out in order to prepare particles to be used as rare-earth doped Y_2O_3 and YAG polycrystalline transparent ceramic for laser source applications.

© 2009 Elsevier Ltd and Techna Group S.r.l. All rights reserved.

Keywords: Ceramic nanomaterials; Laser; Microwave synthesis; Polyol; Doping; Water processing

1. Introduction

Synthesis of sub-micrometer non-agglomerated Yttria particles is of great interest to produce devices for laser sources ($\text{Y}_3\text{Al}_5\text{O}_{12}$, yttrium aluminium garnet, YAG). In view of this application, ceramic materials must have optical qualities, comparable with that of commercial high-quality doped-YAG single crystals. Unfortunately, conventional polycrystalline ceramic materials have many light-scattering centres (refractive index modulation around the grain boundary; refractive index change by inclusions or after sintering residual pores and segregation of different phases) that can affect lasing ability [1]. To decrease the derived optical loss, it is extremely important to fabricate fully dense ceramics with a pore-free structure. This can be obtained when the raw powders, that will be sintered to obtain the polycrystalline ceramic material, are non-agglomerated, of round shape and nanometric size [2–6]. The common chemical

methods used to prepare nano-oxides pass through the hydrolysis of precursors salts (nitrate or organometallic species) followed by condensation and separation of a solid phase [7]. A crucial step of the synthesis is the formation of nuclei big enough to separate from the solvent in form of solid phase (nucleation). The simplest method for the generation of uniformly sized colloidal metal oxides is based on forced hydrolysis of metal salt solutions. The abrupt increasing of temperature and the controlled release of hydrolysing agent at high temperature (water) accelerate the hydrolysis and ensure a fast nucleation followed by a diffusion controlled growth of nuclei. The result is the desiderate formation of particles with an homogeneous distribution of size, shape and degree of crystallinity [8,9]. Polyol method, based on the direct precipitation in a high boiling alcohol such as DEG [10–12] with microwave-assisted heating [13–17] looks a very promising method to prepare powder for fully dense sintered materials and to easily dope yttria with the desired amount of Yb^{3+} . In this paper we describe the synthesis and characterization of Y_2O_3 and Yb^{3+} doped Y_2O_3 sub-micrometer powder from nitrate precursors by microwave-assisted polyol process.

^{*} Corresponding author. Tel.: +39 0546 699 732; fax: +39 0546 46381.

E-mail address: marina.serantoni@istec.cnr.it (M. Serantoni).

2. Experimental procedure

2.1. Instruments

The microwave system used was a Milestone Micro-SYNTHplus. The microwave power is generated by 2×800 W magnetron, with frequency 2.450 GHz.

Phase purity was tested by X-ray diffractometer (XRD) with a Miniflex Rigaku (Japan) system operating with Ni filtered Cu K α radiation. Infrared spectra were recorded in the range 400–4000 cm $^{-1}$, using a Fourier transform infrared spectrometer (FTIR) (PerkinElmer 1700). Inductively coupled plasma-atomic emission spectrometry (ICP-AES) (Liberty 200, Varian, Clayton South, Australia) was used to check the stoichiometry of the doped sample. Thermo-gravimetry (TG)–differential scanning calorimetry (DSC) were carried out at a heating rate of 10 °C/min using a simultaneous thermal analyzer (STA 449, Netzsch, Selb/Bavaria, Germany). Powder morphology was investigated by scanning electron microscopy (SEM) (Leica Cambridge Stereoscan 360) coupled with an energy-dispersive X-ray spectrometer (EDX).

2.2. Synthesis and calcination of the samples

For the synthesis of Y $_2$ O $_3$, yttrium nitrate (Y(NO $_3$) $_3 \times 4$ H $_2$ O, Aldrich 99.99%) was added to diethylene glycol (DEG) (Alfa-Aesar 99%); whereas ytterbium nitrate (Yb(NO $_3$) $_3 \times 5$ H $_2$ O, Aldrich 99.999%) was added together with yttrium nitrate into the reaction vessel containing DEG to obtain Yb–Y $_2$ O $_3$. Forced hydrolysis of the dissolved precursors was obtained by addition of water (Ultrapure Millipore 18 M Ω cm), when the solution reached 140 °C. Reaction products were formed during subsequent heating at 170 °C for 2 h, see Table 1. The Y $_2$ O $_3$ synthesis product was separated from the solvent by centrifugation, washed three times by ethylic alcohol then dried at 100 °C for 2 h in oven. It was calcined at 800 °C for 30 min to obtain a white and crystalline material. SEM analysis of the Y $_2$ O $_3$ powder show that the desired non-agglomeration of particles was not fully obtained. In order to overcome this problem, the Yb–Y $_2$ O $_3$ synthesis products were treated in a different way. Powder was separated from the solvent by sedimentation and it was washed three times in ethylic alcohol and three times in ultrapure water. Separation from the washing liquid was always done by sedimentation. The washed powder was then freeze dried. XRD analysis showed that it was amorphous. The freeze dried powder was calcined at 650 °C, for 30 min to obtain a crystalline material.

Table 1
Microwave-assisted heating power-temperature ramp.

	Time	Power	Temperature	
A	5 min	300 W	140 °C	DEG + precursors
B	20 min	150 W	140 °C	Add. of water
A	22 min	180 W	170 °C	–
B	2 h	210 W	170 °C	–

A: power–temperature ramp; B: temperature plateau.

3. Results and discussion

3.1. ICP analysis of the doped sample

The ratio of precursors in the reaction vessel was calculated in order to obtain a theoretical 9.8% Yb doping of the Ytria powder. This corresponds to Yb–Y $_2$ O $_3$ with ideal stoichiometry of Yb $_{0.196}$ Y $_{1.804}$ O $_3$. ICP analysis performed on powder calcined at 650 °C gave a stoichiometry of Yb $_{0.227 \pm 0.008}$ Y $_{1.77 \pm 0.06}$ O $_3$ (Yb 11.35%), with the ytterbium amount slightly higher of what expected from the precursors rate. This could be explained as due to higher solubility of yttrium then ytterbium synthesis products in water due to the higher atomic radius of yttrium that favour the yttrium oxide-hydroxide dissolution in water [18].

3.2. TG–DSC analysis

TG–DSC analysis were performed in order to define the calcination temperature of the as-synthesized powders. Fig. 1 shows graphs related to Y $_2$ O $_3$ synthesis products washed by ethylic alcohol and water, and ethylic alcohol only. All DSC curves showed two exothermic reactions from 300 to 500 °C that are attributed to nitrates and DEG by-product combustion. For the Y $_2$ O $_3$ washed by ethylic alcohol an endothermic reaction is detected at 750 °C associated with the 8.7% of weight loss. When this sample was calcined at 500 °C, it gave origin to a dark gray colored powder. The graph obtained by FTIR analysis of this powder showed two large bands centered at 1400–1600 cm $^{-1}$, indicating the presence of organic material. The graph related to XRD analysis was composed by very broad peaks of weak intensity that indicated a low level of crystallization. The powder calcined at 800 °C for 30 min was of white color. FTIR and XRD analysis showed that there was no presence of organic material and that the material was crystalline. This strongly suggests that the endothermic peak at 750 °C is related to the transition from amorphous to crystalline material.

It is worth to notice that for samples washed by both ethylic alcohol and water this amorphous/crystalline transformation is shifted at 600, 150 °C lower than for sample washed by ethylic

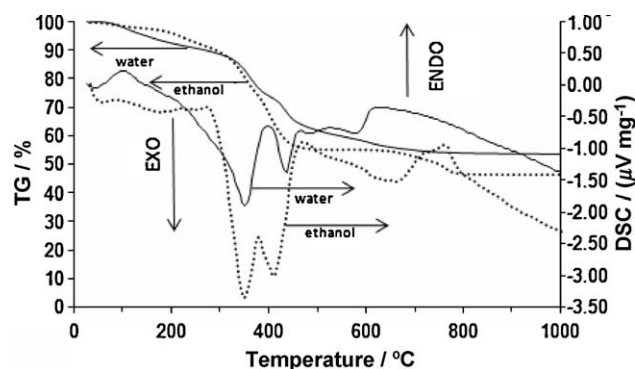


Fig. 1. TG–DSC analysis. Thermal behavior of Y $_2$ O $_3$ samples due to different washing: ethylic alcohol only (ethanol: dotted lines); ethylic alcohol and ultrapure water (water: full lines). Water treatment decreased the calcination temperature of 150 °C.

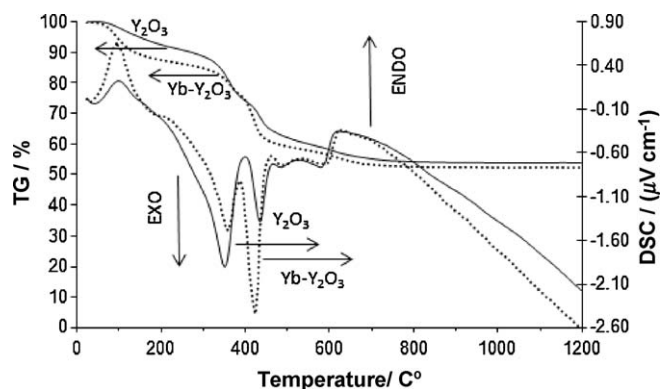


Fig. 2. TG–DSC analysis. Thermal behavior of Y_2O_3 and $\text{Yb-Y}_2\text{O}_3$ samples washed by ethylic alcohol and water. No effect is detected due to Yb-doping.

alcohol only and this transition is associated to a lower (2.7%) weight loss. From this data it is possible to assume that washing by water produces the dissolution of DEG by-products present on the powder and this allows the crystallization of the sample at a lower temperature.

Y_2O_3 and $\text{Yb-Y}_2\text{O}_3$ powders washed by both ethylic alcohol and water, were compared to verify the effect of the Yb doping on the thermal behavior (Fig. 2). There was no thermal effect due to the presence of Yb into the synthesized powder.

3.3. XRD analysis

Fig. 3 displays the XRD patterns of the two samples after calcination. Both samples showed the diffraction typical of the cubic structure of yttrium oxide (JCPDF 41-1105). A narrow range of 2θ was selected to detect the effect of Yb on the crystalline lattice of Y_2O_3 and verify the presence of doping. The average shift of 0.5, 2θ degrees toward ytterbium oxide diffraction pattern (JCPDF 41-1106) confirms the insertion of Yb atoms in the crystal lattice. Peaks of $\text{Yb-Y}_2\text{O}_3$ were always less intensive and with a larger base than in the pure Y_2O_3 pattern, even for XRD analysis performed on samples calcined at higher temperatures. This can indicate the presence of stress and disorder induced by the presence of ytterbium atoms in the crystal lattice of Y_2O_3 or can only be due to the smallest size of $\text{Yb-Y}_2\text{O}_3$ particle (150–200 nm) in respect to Y_2O_3 particles (200–250 nm). The small difference in cell parameters (from Rietveld Analysis of XRD data) of the synthesized sample from

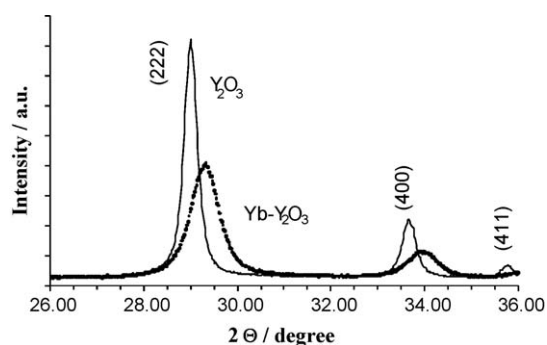


Fig. 3. XRD patterns of Y_2O_3 calcined at 800 °C (full line); $\text{Yb-Y}_2\text{O}_3$ calcined at 650 °C (dotted line).

Table 2

Cell parameters of yttria powders (Rietveld method).

Sample	a (Å)	Particle size (nm)
Y_2O_3 DEG	10.6085	200–250
$\text{Yb-Y}_2\text{O}_3$ DEG	10.5971	150–200
Y_2O_3 (JCPDF 41-1105)	10.6041	–
Yb_2O_3 (JCPDF 41-1106)	10.4347	–

the tabulated value (10^{-2} unit on 10 = 1×10^{-3} , see Table 2), does not justify the difference in particle size (50 unit on 200 = 0.25), measured by SEM images, between the doped and un-doped yttria particles. The smaller particle size of Yb doped sample could be due to lattice defect such as oxygen substoichiometry and to a lower particles growing rate in respect to the un-doped case.

3.4. FTIR analysis

FTIR analysis showed that as-synthesized samples contain organic phases as DEG and nitrate reaction by-products. In Fig. 4 the FTIR graphs of $\text{Yb-Y}_2\text{O}_3$ powder, as-synthesized, after water washing and after calcination are reported. The intense bands at 1600 cm^{-1} and at 1384 cm^{-1} are related to the stretching (symmetric and anti-symmetric) of the NO group bonded to an aliphatic carbon atom. The presence of DEG by-products (acetaldehyde and diacetyl [7,14]) is clearly showed by the bands at 2926 and 1448 cm^{-1} due to CH stretching and bending. 1415 – 1327 and 726 – 768 cm^{-1} bands are due to the bending (in and out of plane) of OH groups, whereas bands at 1110 and 925 cm^{-1} are attributed to the symmetric stretching of the C–O–C group. The water washing removes a good amount of DEG and nitro by-products and, as a consequence, in the FTIR spectrum of sample treated by water the bands centered at 1100 , 1400 , 2900 cm^{-1} are remarkably weak. This effect is confirmed also by the thermal analysis indicating that the water treatment eliminates a good amount of DEG by-products such that the weight thermal loss in that samples is much lower than for “ethylic alcohol only” washed samples (Fig. 2). After calcination the FTIR spectra do not show absorption due to the presence of organic products in the sample. An intense band is visible at 500 – 600 cm^{-1} , characteristic of the metal–oxygen bond.

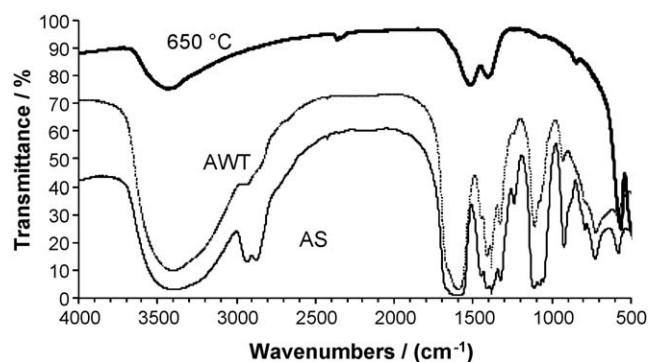


Fig. 4. FTIR spectra of as-synthesized $\text{Yb-Y}_2\text{O}_3$: as synthesized (AS: full line); after water treatment (AWT: dotted line); after calcination at 650 °C (thick line).

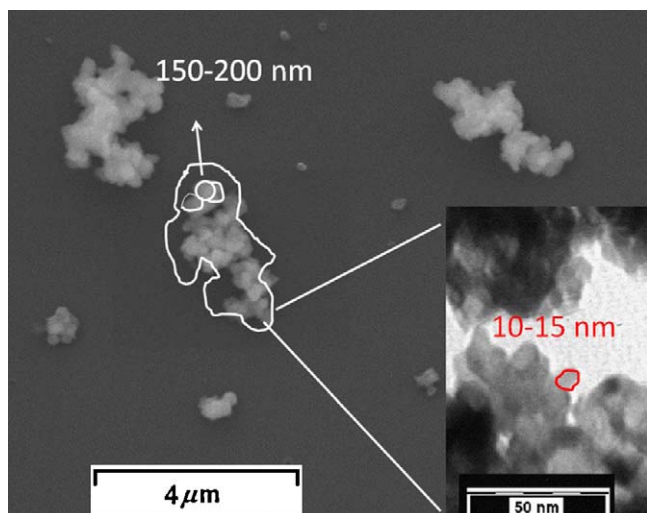


Fig. 5. SEM and TEM (insert) images Yb- Y_2O_3 powder after calcination at 650 °C. It is showed the different level of nanostructure organization: from nanocrystals (10–15 nm) to primary particles (150–200 nm) to micrometer aggregates (2–4 μm).

3.5. SEM and EDS analysis

Fig. 5 shows a SEM image of the powder Yb- Y_2O_3 calcined at 650 °C.

Particles have a round shape, with diameter of ~ 150 nm. The samples is composed by monodisperse particles and small agglomerates of different sizes (from 1 to 10 μm) that look soft and without the presence of sintering necks. This scarce agglomeration is due to the freeze drying treatment. Preliminary TEM analysis showed that each particles is formed by nanocrystallites of about 10–15 nm in size (insert in Fig. 5) and EDX analysis showed an uniform distribution of Yb in the doped powder.

4. Conclusion

This paper reports the description of a synthesis of yttria and ytterbium-doped yttria powders by a combination of two process: microwave-assisted heating method and polyol (DEG) synthesis, from nitrate precursors. The reaction products washed by ultrapure water showed a decrease of 150 °C in the calcination temperature for phase formation, in respect to the product washed by ethylic alcohol only. Powders were characterized by different techniques and the results showed that they have the correct requirements for the fabrication of laser optical devices. In the case of Yb- Y_2O_3 , ytterbium atoms entered the nanocrystals lattice, in percentage very close to the initial precursor ratio.

Acknowledgments

Work funded by IFAC-CNR in the frame of IFAC-RSTL-CNR (Ricerca spontanea a Tema libero) Number 959: “Nuovi promettenti mezzi attivi drogati ad Ytterbio per laser tunabili nel vicino infrarosso”, under the supervision of Dr. Matteo Vannini in collaboration with ISTEC-CNR.

References

- [1] A. Ikesue, Y.L. Aung, T. Taira, T. Kamimura, K. Yoshida, G.L. Messing, Progress in ceramic lasers, *Annu. Rev. Mater. Res.* 36 (2006) 397–429.
- [2] J. Mouzon, C. Dujardin, O. Tillement, M. Oden, Synthesis and optical properties of $\text{Yb}_{0.6}\text{Y}_{1.4}\text{O}_3$ transparent ceramics, *J. Alloys Compd.* 464 (2008) 407–411.
- [3] A. Ikesue, Y.L. Aung, T. Yoda, S. Nakayama, T. Kamimura, Fabrication and laser performance of polycrystal and single crystal Nd:YAG by advanced ceramic processing, *Opt. Mater.* 29 (2007) 1289–1294.
- [4] J. Mouzon, P. Nordell, A. Thomas, M.J. Oden, Comparison of two different precipitation routes leading to Yb doped Y_2O_3 nano-particles, *J. Eur. Ceram. Soc.* 27 (2007) 1991–1998.
- [5] J. Mouzon, T. Lindback, M.J. Oden, Influence of agglomeration on the transparency of yttria ceramics synthesis and performance of advanced ceramic lasers, *J. Am. Ceram. Soc.* 91–10 (2008) 3380–3387.
- [6] A. Ikesue, Y.L. Aung, Synthesis and performance of advanced ceramic lasers, *J. Am. Ceram. Soc.* 89 (2006) 1936–1944.
- [7] J. Livage, Sol–gel synthesis of heterogeneous catalysis from aqueous solutions, *Catal. Today* 41 (1998) 3–19.
- [8] C. Guozhong, *Nanostructures & Nanomaterials*, Imperial College Press, London, 2004, pp. 51–93.
- [9] V. La Mer, R.H. Dinegar, Theory, production and mechanism of formation of monodispersed hydrosols, *J. Am. Chem. Soc.* 72–11 (1950) 4847–4854.
- [10] F. Fievet, J.P. Lagier, B. Blin, B. Beaudoin, M. Figlarz, Homogeneous and heterogeneous nucleation in the polyol process for the preparation of micron and sub-micron size metal particles, *Solid State Ionics* 32–33 (1989) 198–205.
- [11] I.R. Collins, S.E. Taylor, Non-aqueous thermal decomposition route to colloidal inorganic oxides, *J. Mater. Chem.* 2 (1992) 1277–1281.
- [12] D. Jezequel, J. Guenot, N. Jouini, F.J. Fievet, Submicrometer zinc-oxide particles—elaboration in polyol medium and morphological characteristics, *Mater. Res.* 10 (1995) 77–83.
- [13] C. Feldmann, Polyol-mediated synthesis of nanoscale functional materials, *Solid State Sci.* 7 (2005) 868–873.
- [14] M.A. Flores-Gonzalez, G. Ledoux, S. Roux, K. Lebbou, P. Perriat, O. Tillement, Preparing nanometer scaled Tb-doped Y_2O_3 luminescent powders by the polyol method, *J. Solid State Chem.* 178 (2005) 989–997.
- [15] O. Palchik, J.J. Zhu, A.J. Gedanken, Microwave assisted preparation of binary oxide nanoparticles, *J. Mater. Chem.* 10 (2000) 1251–1254.
- [16] T. Nakamura, S. Yanagida, Y. Wada, Preparation of nano-sized YAG: Eu³⁺ particles by a microwave-assisted polyol process and their luminescence properties, *Res. Chem. Intermed.* 32 (2006) 331–339.
- [17] S.E. Skrabalak, B.J. Wiley, M. Kim, E.V. Formo, Y.N. Xia, On the polyol synthesis of silver nanostructures: glycolaldehyde as a reducing agent, *Nano Lett.* 8 (2008) 2077–2081.
- [18] M. Nagao, H. Hamano, K. Hirata, R. Kumashiro, Y. Kuroda, Hydration process of rare-earth sesquioxides having different crystal structures, *Langmuir* 19 (2003) 9201–9209.